FILTRATION OF AN AQUEOUS SALT SOLUTION IN CAPILLARY-POROUS MATERIALS IN THE PRESENCE OF A PHASE TRANSITION

P. A. Novikov, A. V. Kuz'mich,
and L. A. Sergeeva

UDC 621.47

The position of the saturation boundary of an aqueous salt solution during filtration and salinization of capillary-porous wicks is determined as a function of density of the incident thermal flux.

The productivity of portable solar stills is determined to a certain extend by the efficiency of its evaporator, which also performs the function of a capillary-porous wick [1, 2]. As a result of combined filtration and evaporation processes in such apparatus distilled water is produced.

With increase in the density of the thermal flux toward the evaporator surface the output of distillate from the device is increased, but at the same time the salt concentration in the solution increases more rapidly, causing earlier saturation and salinization of the evaporator.

The goal of the present study is to investigate the processes of filtration and saturation of an aqueous NaCl solution, the concentration of which varies due to evaporation of water from the surface of the capillary-porous material. Experiments were performed on model wicks with various orientations in the gravitational field.

A special experimental device was developed for the studies (Fig. 1). The wicks 1 were cut from filter paper and composition material containing cellulose and Lavsan (40%), 0.2 mm thick. The wicks were installed in trays with holders having a positioner 2 to regulate the angle of the wick to the horizontal. One end of the wick contacted a 10% H_2O + NaCl solution which was poured into reservoir 3 through spigot 4, with excess solution flowing into basin 5 from the other end of the device. The tray was sealed on top by a glass plate 6, upon which water evaporated from the wick condensed, and closed at both ends by thermal insulation 7. The distillate was collected in the collector vessel 8. Fan 9 was used to improve cooling of the condenser. A radiant flux to the wick was generated by radiation source 10, consisting of two type DKsT-5000 xenon arc lamps mounted in a protective cover 11 with mirror reflectors, thermal insulators, and lamp screens cooled by air flow. The radiant power level was adjusted by the electronic regulator 12 and recorded by a pyranometer and galvanometer. Positioner 13 was used to adjust the lamps to a position parallel to the plane of the wick. Surface temperatures of the wick and condenser were monitored with microthermocouples 14 and switch 15.

It was found in studying the filtration and evaporation processes that salinization of the wick occurred nonuniformly over its section. Upon saturation of the solution salt precipitated on the planar wick surface first at the edges, then over the entire filtration front (Fig. 2).

There are several causes of this edge effect. A capillary-porous wick consists of a set of chaotically distributed communicating capillaries of variable section. Open capillaries occur at the edge of the wick, in the mouths of which liquid halts during evaporation, forming static meniscuses. Since wetting angles are different at the edge and within the wick, i.e., the filtration front is not a surface of uniform pressure, the condition of filtration front rectilinearity is disrupted at the edge [3].

The component of the solution flow velocity perpendicular to the direction of motion of the filtration front vanishes at the edge of the wick, so that the liquid layer formed by the liquid meniscuses at the wick edge will brake the layer behind it, etc. As a result the

---

A. V. Lykov Heat and Mass Transport Institute, Academy of Sciences of the Belorussian SSR, Minsk. Translated from Inzhenerno-Fizicheskii Zhurnal, Vol. 52, No. 2, pp. 271-276, February, 1987. Original article submitted February 14, 1986.

0022-0841/87/5202-0205$12.50

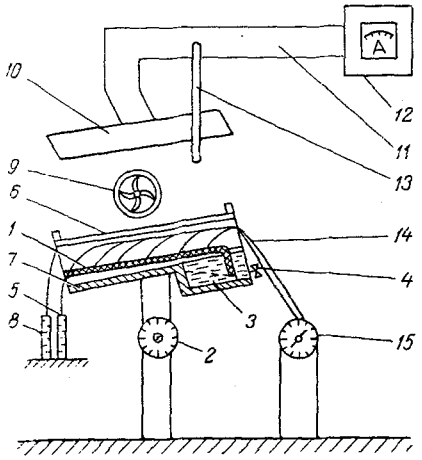

Fig. 1. Diagram of experimental apparatus.

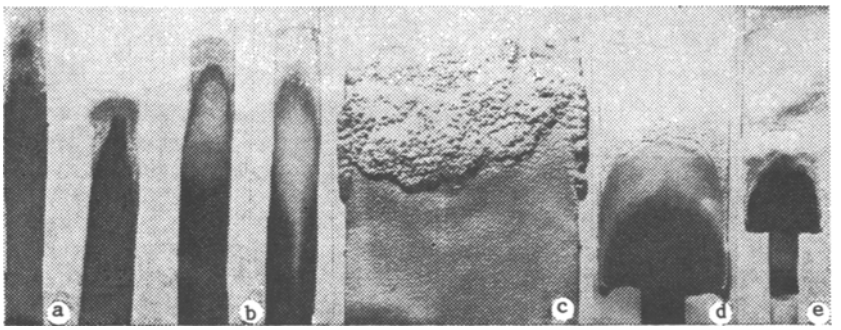

Fig. 2. Edge effects in wick salinization occurring during filtration of 10% salt solution: a, c, d) filter paper; b, e) composition material; a, b, width 10-15 mm; d, e, variable width (absorption time 6 h); c, width 120 mm (absorption time 3 days).

solution flow rate near the edges will be less than within the wick, and saturation of the solution in this region should occur earlier.

Consequently, one cause of the edge effect in salinization is the development of a filtration rate gradient at the wick edges. It should be noted that this effect appears to a greater degree at low filtration rates, i.e., at the completion of the absorption process, when equalizing forces affecting the filtration begin to appear.

A second cause of nonuniform salinization of the wick over its section is evaporation of the solution from the open pores at the wick edges. To clarify the importance of additional evaporation from the wick edges to salt crystal growth during salinization the following experiments were performed. Two identical rectangular specimens were cut from filter paper and each was divided into four equal segments. The two end segments of one specimen were saturated with distilled water, while the two central segments of the other were similarly saturated. The specimens were then suspended from an analytic balance and the water evaporation rate determined from the change in weight with time. It was found that this rate was higher for wetting of the end segments, a consequence of additional evaporation from the two open ends of the specimen.

Thus, in filtration of an aqueous salt solution, because only one component of the solution – the water – evaporates from the wick surface, and additional evaporation occurs from the edge surfaces, the salt concentration in the solution at the wick edges increases more rapidly than at the center, which then leads to more intense growth of salt crystals in these portions of the wick (Fig. 2).

In order to calculate the position of the solution saturation and wick salinization boundary, it is necessary to know the distribution of solution flow rate and concentration over wick length. We will consider the flow rate of the H_2O + NaCl solution formally as the sum of the flow rates of its components:

$$g(l) = g_{H_2O} + g_{NaCl}. \qquad (1)$$

During evaporation the solution concentration increases and at some distance ℓ_{sat} becomes saturated. The specific flow rate of the solution $g(\ell)$ then decreases from its initial value g_0, at which the condentration is equal to c_0, to some value g_{sat} with concentration c_{sat}, corresponding to saturation. Assuming that the rate of water evaporation from the solution is constant in time and uniformly distributed over the wick surface, for each position of the filtration front we can write the following balance equation:

$$g(l) = g_0 - j_m l/h. \tag{2}$$

Here the evaporation rate j_m is referred to a wick surface of length ℓ. Considering that the specific solution flow rates g_0 and j_m do not depend on ℓ, from Eq. (2) we determine the position of the filtration front boundary as a function of solution flow rate $g(\ell)$:

$$l = \frac{g_0 - g(l)}{j_m} h. \tag{3}$$

We can now transform from Eq. (3) to the dependence of ℓ on solution concentration. Since the specific flow rate g_{NaCl} is constant over the length of the wick, from the formal equality (1) we obtain

$$c(l) = \frac{g_{NaCl}}{g(l)}, \quad c_0 = \frac{g_{NaCl}}{g_0}, \quad c_{sat} = \frac{g_{NaCl}}{g_{sat}}. \tag{4}$$

The specific solution flow rate produced by water evaporation from the wick surface for various thermal fluxes can be written as:

$$j_m = \frac{kq}{L}, \tag{5}$$

where k is an efficiency coefficient, equal to the ratio of the quantity of heat expended in the phase transition of solution evaporation per unit time to the total thermal flux incident on the wick. The value of k was determined experimentally from the quantity of distillate collected in vessel 8 per unit time. The average value of k, calculated from thermal flux and solution flow rate values, measured over 10 h of operation, was equal to 0.37.

Substituting Eqs. (4) and (5) in Eq. (3), we obtain an expression for determination of the position of the solution saturation boundary

$$l_{sat} = \frac{g_0 (1 - c_0/c_{sat})}{kq} L_{sat} h, \tag{6}$$

where L_{sat} is the latent heat of evaporation of a solution with concentration c_{sat}.

To find the solution specific flow rate g_0 in the input portion of the wick (i.e., without evaporation) at any moment in time it is necessary to determine the time dependence of solution filtration front velocity. To do this we can use Washborn's equation [4]

$$\frac{l_f}{l_\infty} + \ln\left(1 - \frac{l_f}{l_\infty}\right) = -\frac{\sigma(c) r \cos\Theta}{4\eta l_\infty^2} t, \tag{7}$$

where

$$l_\infty = \frac{2\sigma(c)\cos\Theta}{r\rho g \sin\alpha},$$

or the expression for capillary saturation of porous materials obtained by Deryagin [4]:

$$l_f = \beta t^{1/2}, \tag{8}$$

where

$$\beta = \frac{2K\rho\sigma(c)\cos\Theta}{\eta\varepsilon}.$$

But in order to calculate velocities with Eqs. (7), (8) it is necessary to know the permeability, the surface tension of the solution with the paper, and other physical quantities, data on which are not available in the literature, and exact experimental determination of

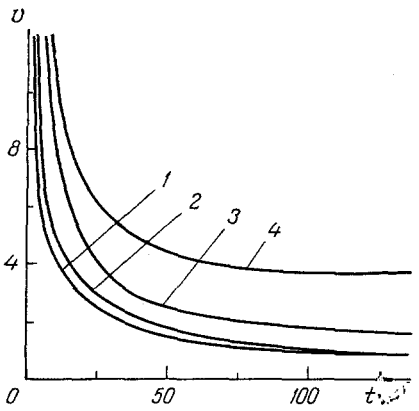

Fig. 3

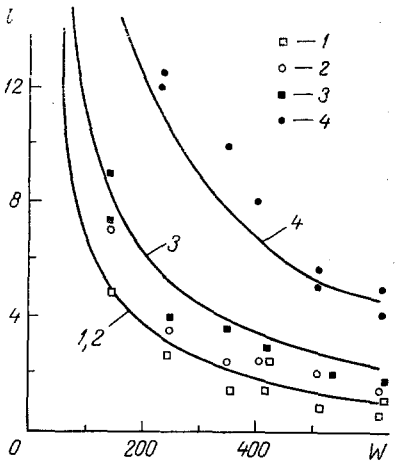

Fig. 4

Fig. 3. Filtration front velocity vs saturation time: 1, 2) vertical wick position; 3, 4) horizontal; 1, 3) filtration paper; 2, 4) composition material. $v \cdot 10^5$, m/sec; $t \cdot 10^{-2}$, sec.

Fig. 4. Solution saturation and wick salinization front boundary position vs thermal flux density. Curves, calculation with Eq. (9); points, experimental data. Numbers 1-4 as in Fig. 3. $\ell \cdot 10^2$, m; W, W/m^2.

which is extremely complicated. The time dependence of the filtration front velocity $v_f = f(t)$ was measured experimentally for horizontal and vertical wick positions (Fig. 3). In order to eliminate evaporation during the filtration process the wick was placed between two transparent polymer films.

Using the function $v_f = f(t)$ thus obtained and considering the continuity equation div $v_f = 0$, we find the initial flow rate g_0 as the product of v_f at time t times the density of the 10% NaCl solution.

Thus, the final expression for determination of the position of the solution saturation and wick salinization boundary takes on the form

$$l_{sat} = \frac{v_f \rho (1 - c_0/c_{sat})}{kq} L_{sat} h. \qquad (9)$$

Calculation with Eq. (9) and comparison with experiment (Fig. 4) were performed for a 3.5 h saturation time. Since the salt is nonvolatile, neglecting the dependence of L on concentration, the latent heat of evaporation of the solution was taken equal to the latent heat of evaporation of water. Values of c_{sat} and L for the corresponding temperatures were taken from [5].

As is evident from Fig. 4, on the whole the calculation agrees satisfactorily with experiment. Deviation of the experimental points from Eq. (9) can be explained by the inexact determination of the position of the solution saturation boundary, related to the edge effect described above and the absence of a rectilinear wick salinization profile, as well as certain assumptions made in deriving the expression.

Thus, using Eq. (9) and considering nonuniformity of the salinization of the capillary-porous material related to the edge effect, approximate estimates can be made of the length at which salinization will not occur, and recommendations can be made for wick selection in portable solar stills.

NOTATION

g_0, $g(\ell)$, g_{sat}, specific flow rate of aqueous salt solution at input to wick and distances ℓ and ℓ_{sat} from wick input; j_m, specific flow rate of water evaporating from wick solution; c_ℓ, $c(\ell)$, c_{sat}, salt solution concentrations at input to wick and distances ℓ and ℓ_{sat} from wick input; S, h, b, cross sectional area, thickness, and width of wick; q, specific thermal flux; L, latent heat of evaporation of water from the solution; ℓ_f, v_f, position and velocity of filtration front; ε, K, porosity and permeability of capillary-porous wick; $\sigma(c)$,

η, ρ, solution surface tension, viscosity, and density; Θ, limiting wetting angle; r, mean pore radius; g, acceleration of gravity; α, inclination of wick to horizontal.

LITERATURE CITED

1. V. I. Novikova, Geliotekhnika, No. 2, 44-48 (1984).
2. P. A. Novikov, V. I. Novikova, and E. K. Snezhko, Vests. Akad. Nauk BSSR, Ser. Fiz.-Energ. Navuk, No. 2, 90-96 (1985).
3. R. Collins, Liquid Flow through Porous Materials [Russian translation], Moscow (1964).
4. G. A. Aksel'rud and M. A. Al'tshuler, Introduction to Capillary-Chemical Technology [in Russian], Moscow (1983).
5. G. W. Kaye and T. H. Laby, Tables of Physical and Chemical Constants, Longman (1973).

A COMPARISON OF METHODS OF COMBINING FORCE PARAMETERS

A. N. Berezhnoi and V. N. Shekurov

UDC 533.15

A study is made of two models for the molecular-interaction potential in calculating diffusion coefficients for binary vapor–gas systems.

One needs information on diffusion coefficients (DC) for binary vapor–gas systems for calculations on chemical engineering processes [1], so one needs methods of forecasting DC. The kinetic theory of gases gives DC from the following equation [2-4]:

$$D_t = \frac{1{,}883\,(10)^{-24}\sqrt{T^3\left(\frac{1}{M_1}+\frac{1}{M_2}\right)}}{p\sigma_{12}^2\Omega_D}, \tag{1}$$

where the combination relations used are [2-9]:

$$\sigma_{12} = (\sigma_1+\sigma_2)/2,\ \varepsilon_{12} = (\varepsilon_1\varepsilon_2)^{1/2}; \tag{2}$$

$$\sigma_{12} = (\sigma_1+\sigma_2)/2,\ \varepsilon_{12} = (\varepsilon_1\sigma_1^6\varepsilon_2\sigma_2^6)^{1/2}/\sigma_{12}^6; \tag{3}$$

$$\sigma_{12} = (\sigma_1+\sigma_2)/2,\quad \varepsilon_{12} = 2\varepsilon_1\varepsilon_2/(\varepsilon_1+\varepsilon_2); \tag{4}$$

$$\sigma_{12} = (\sigma_1+\sigma_2)/2,\ \varepsilon_{12}\sigma_{12}^{12} = \frac{\varepsilon_1\sigma_1^{12}}{2^{13}}\left[1+\left(\frac{\varepsilon_2\sigma_2^{12}}{\varepsilon_1\sigma_1^{12}}\right)^{1/13}\right]^{13}; \tag{5}$$

$$\sigma_{12}^6\varepsilon_{12} = (\varepsilon_1\sigma_1^6\varepsilon_2\sigma_2^6)^{1/2},\ \varepsilon_{12}\sigma_{12}^{12} = \frac{\varepsilon_1\sigma_1^{12}}{2^{13}}\left[1+\left(\frac{\varepsilon_2\sigma_2^{12}}{\varepsilon_1\sigma_1^{12}}\right)^{1/13}\right]^{13}. \tag{6}$$

We have calculated DC for two molecular interaction potentials: the 6-12 Lennard-Jones one and the Kessel'man effective potential [7]. The collision integral Ω_D is defined by [3]

$$\Omega_D = \frac{A}{(T^*)^B} + \frac{C}{\exp ET^*} + \frac{G}{\exp FT^*} + \frac{L}{\exp HT^*}, \tag{7}$$

where $T^* = kT/\varepsilon_i$; A = 1.06036; B = 0.15610; C = 0.19300; E = 0.47635; G = 1.03587; F = 1.52996; L = 1.76474; H = 3.89411. The values of σ_i and ε_i for pure substances were taken from the literature for the first model (Table 1), while for the second they were determined graphically from [7]. Figure 1 shows the results. The deviations are given by

Kirov Kazan Chemical Engineering Institute.

Translated from Inzhenerno-Fizicheskii Zhurnal, Vol. 52, No. 2, pp. 276-281, February, 1987. Original article submitted December 10, 1985.